

Temperature-dependent IR spectroscopic and structural study of 18-crown-6 chelating ligand in the complexation with sodium surfactant salts and potassium picrate

Tea Mihelj^{1*}, Vlasta Tomašić¹, Nikola Biliškov², Feng Liu³

¹*Department of Physical Chemistry, Ruđer Bošković Institute, POB 180, HR-10002 Zagreb, Croatia*

²*Division of Organic Chemistry and Biochemistry, Ruđer Bošković Institute, POB 180, HR-10002 Zagreb, Croatia*

³*State Key Laboratory for Mechanical Behavior of Materials, Xi'an Jiaotong University, Xi'an 710049, China*

*
Corresponding Author:

Email: tmihelj@irb.hr

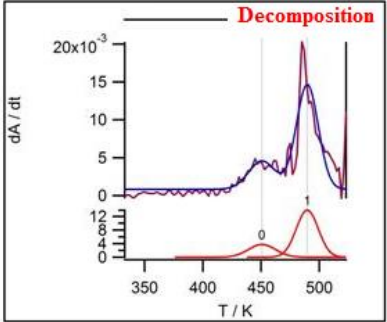
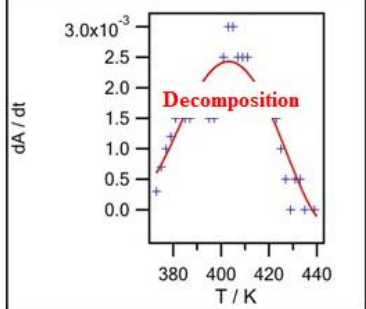
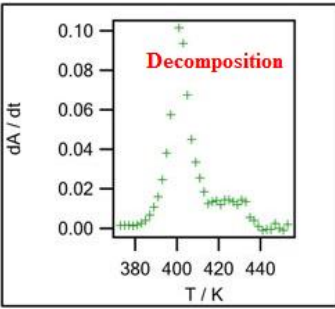
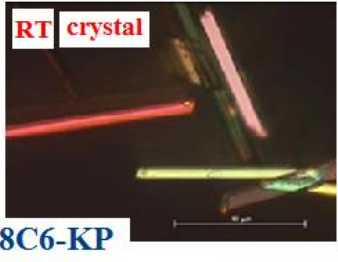
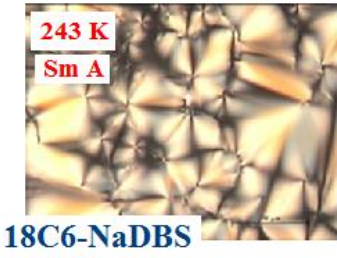
Ruđer Bošković Institute, Department of Physical Chemistry, Laboratory for synthesis and processes of self-assembling of organic molecules, Bijenička c. 54

P.O. Box 180, HR-10002 Zagreb, Croatia

Fax: +38514680245

Tel: +38514571211

Graphical abstract



Abstract

18-crown-6 ether (18C6) complexes with the following anionic surfactants: sodium *n*-dodecylsulfate (18C6-NaDS), sodium 4-(1-pentylheptyl)benzenesulfonate (18C6-NaDBS); and potassium picrate (18C6-KP) were synthesized and studied in terms of their thermal and structural properties. Physico-chemical properties of new solid 1:1 coordination complexes were characterized by infrared (IR) spectroscopy, thermogravimetry and differential thermal analysis, differential scanning calorimetry, X-ray diffraction and microscopic observations. The strength of coordination between Na⁺ and oxygen atoms of 18C6 ligand does not depend on anionic part of the surfactant, as established by thermodynamical parameters obtained by temperature-dependent IR spectroscopy. Each of these complexes exhibit different kinds of endothermic transitions in heating scan. Diffraction maxima obtained by SAXS and WAXS, refer the behavior of the compounds 18C6-NaDS and 18C6-NaDBS as smectic liquid crystalline. Distortion of 18C6-NaDS and 18C6-KP complexes occurs in two steps. Temperature of the decomplexation of solid crystal complex 18C6-KP is considerably higher than of mesophase complexes, 18C6-NaDS, and 18C6-NaDBS. The structural and liquid crystalline properties of novel 18-crown-ether complexes are function of anionic molecule geometry, type of chosen cation (Na⁺, K⁺), as well as architecture of self-organized aggregates. A good combination of crown ether unit and amphiphile may provide a possibility for preparing new functionalized materials, opening the research field of ion complexation and of host-guest type behavior.

Keywords: 18-crown-6 ether, IR spectroscopy, X-ray diffraction, anionic surfactants, thermal properties, liquid crystals

1 Introduction

Several molecular families have been widely examined for the development of supramolecular chemistry. The group of macrocyclic polyethers, known as crown ethers, have become valuable tools in organic synthesis due to their ability to solvate alkali, alkaline-earth, transition-metal, and ammonium cations [1–4]. Their selective cation binding makes them applicable for different environmental usage [5,6], drug delivery [7,8], recovery or removal of specific species, models for biological receptors [9], reaction catalysts as well as active sites in ion selective electrodes [10] or chromatographic agents [11]. Alkali metal elements have indispensable role in many biological processes, primarily to be as bulk electrolytes that stabilize surface charges on proteins and nucleic acids [12], and also play unique structural roles in biological systems [13,14]. Their complexes with crown ligands are coordination compounds based on electrostatic interaction through ion-dipole attractions [15], with the usage for simulations of natural substances, their properties and behavior. Some new surfactants derived from crown ethers are used as templates with a particular morphology in the preparation of siliceous mesoporous molecular sieves [16].

One of the most relevant crown ethers, 18-crown-6 (18C6) features a flexible six-oxygen cyclic backbone and uncomplexed does not exhibit any liquid crystalline behavior. However, these phenomena are caused by one or more mesogenic groups attached to the molecules containing crown ether, aza, thia crown ethers, or crown ethers with several different heteroatoms [17–22]. Synthesis and properties of cholesteryl moiety bearing 16-membered crown ethers show cholesteric [23] and nematic [24] liquid crystalline behavior. Thermochemical properties of 18C6 ether complexes with aralkylammonium perchlorates show higher melting points than of both the host and the guest compound, the decomposition begins immediately after melting is completed, and each of the examined complexes is characterized by its individual properties [25]. The study of stable complexes formed between crown ether compounds and surfactants is less explored area, especially in terms of thermochemical and structural studies. So far, most studies on metal ion–crown ether complexes were focused on the determination of relative affinities and stoichiometries of the complexes in solution, rather than on their solid structures. Thus, in the present study we report the formation of defined

complexes between 18C6 and different guest constituent. Two amphiphiles are chosen; one conventional known as sodium *n*-dodecylsulfate and one commercial known as sodium 4-(1-pentylheptyl)benzenesulfonate. The third chosen guest is potassium picrate that possesses hydrophilic-hydrophobic balanced properties, but is not a real amphiphile. The purpose of the present study is to provide an insight into thermal and structural behavior of 18C6 chelating ligand in the complexation with sodium surfactant salts and potassium picrate. Temperature-dependent IR spectroscopy was used in order to detect and characterize phase transitions at molecular level, as well as to determine thermodynamic parameters of the decomplexation process. The present study provides the relationship between molecular structure and physico-chemical properties by combining the properties of complex formation and supramolecular arrangements provided by liquid crystals. This ensures a guideline for further design and fine-tuning of the properties of new materials with a specific structure, allowed by an appropriate choice of cation and crown ether size and by varying the nature of anionic constituent.

2 Experimental

2.1 Materials and sample preparation

18-crown-6 ether, *i.e.* 1,4,7,10,13,16-hexaoxacyclooctadecane ($C_{12}H_{24}O_6$, $M_w/g \text{ mol}^{-1} = 264.32$; Sigma-Aldrich) was used without further purification. Sodium *n*-dodecylsulfate ($C_{12}H_{25}SO_4Na$, $M_w/g \text{ mol}^{-1} = 288.38$) was obtained from Merck and recrystallized several times from ethanol. Sodium 4-(1-pentylheptyl)benzenesulfonate ($C_{12}H_{25}C_6H_4SO_3Na$, $M_w/g \text{ mol}^{-1} = 348.48$) was analyzed and determined previously [26]. Potassium picrate, *i.e.* potassium 2,4,6-trinitrofenolate ($C_6H_2N_3O_7K$, $M_w/g \text{ mol}^{-1} = 267.20$) was prepared and purified according the procedure described earlier [27,28].

18C6 ether complexes with different anionic constituent were prepared by high temperature mixing of equimolar aqueous solutions of both, 18C6 ether and sodium surfactant salt/potassium picrate. The complex formation equilibrium is defined as $M^+ \cdot X^- + L \leftrightarrow ML^+ \cdot X^-$, where M^+ , X^- and L refer to metal ion (Na^+ or K^+), counter anion (*n*-dodecylsulfate, 4-(1-pentylheptyl)benzenesulfonate or picrate), and crown ether as neutral, endopolarophilic ligand. Samples were left aging for few days at room temperature, during which water spontaneously evaporated. 18-crown-6 ether complex with potassium picrate, formed yellow crystals that were filtered and vacuum dried till constant mass was obtained, while other two samples were waxy and after vacuum dried, glassy, colorless and transparent. The samples were stored protected from moisture and light before use.

2.2 Measurements

The complexes are shown in Scheme 1. *Elemental analysis* (Perkin-Elmer Analyzer PE 2400 Series 2) confirmed that the complexes were 1:1 charge ratio adducts. 18C6-sodium *n*-dodecylsulfate (compound **1**, $C_{24}H_{49}SO_{10}Na$, $M_w/g \text{ mol}^{-1} = 552.70$) found: C, 52.18; H, 9.00 % (calc. C, 52.16; H, 8.94 %). 18C6- sodium 4-(1-pentylheptyl)benzenesulfonate (compound **2**, $C_{30}H_{53}SO_9Na$, $M_w/g \text{ mol}^{-1} = 612.80$) found: C, 58.78%; H, 8.70 (calc. C, 58.80; H, 8.72 %). 18C6-potassium picrate (compound

3, $C_{18}H_{26}N_3O_{13}K$, $M_w/g\ mol^{-1} = 531.52$) found: C, 40.60; H, 4.90; N, 7.82% (calc. C, 40.68; H, 4.93; N, 7.91 %).

TG and differential thermal analysis, DTA, were obtained on a Shimadzu DTG-60H. Samples were heated from room temperature to 573 K at the heating rate of $5\ K\ min^{-1}$ in synthetic airflow of $50\ mL\ min^{-1}$. *Differential scanning calorimetry, DSC*, was carried out with a Perkin Elmer Pyris Diamond DSC calorimeter in N_2 atmosphere equipped with a model Perkin Elmer 2P intra-cooler in N_2 atmosphere, at the rate of $2\ K\ min^{-1}$. The transition enthalpy, $\Delta H/kJ\ mol^{-1}$, was determined from the peak area of the DSC thermogram; and the corresponding entropy changes, $\Delta S/J\ mol^{-1}\ K^{-1}$, was calculated using the maximal transition temperature. *Textures* were examined with Leica DMLS polarized optical light microscope, equipped with a Mettler FP 82 hot stage, Sony digital color video camera (SSC-DC58AP). *Infrared transmission spectra* of the solid samples were recorded at $4\ cm^{-1}$ resolution in KBr pellets on an ABB Bomem MB102 single-beam FT-IR spectrometer with CsI optics, DTGS detector. The KBr sample pellets were prepared by mixing $\sim 2\ mg$ of the individual sample with 100 mg of KBr with a pestle and mortar made of agate. Specac 3000 Series high-stability temperature controller with water cooled heating jacket was used to measure the spectra within the temperature range from room temperature up to 523 K under atmospheric conditions and at heating rate of $2\ K\ min^{-1}$ and 2 K steps. Each single-beam spectrum collected in a temperature run for individual sample was ratioed to the single-beam spectrum of the sample-free setup (the reference spectrum) recorded immediately before starting the temperature-dependent measurements. *Wide angle X-ray scattering (WAXS)* results were obtained by automatic powder diffractometer, Philips PW 3710, with monochromatized Cu $K\alpha$ radiation ($\lambda/\text{\AA} = 1.54056$) and proportional counter. The interlayer spacing (d_{hkl}) was calculated according to the Bragg's law. In addition, *small angle X-ray scattering (SAXS)* measurements were made using a MAR Research image plate camera with a rotating anode generated beam doubly focused by multilayer mirrors. Samples were held in Lindeman capillaries temperature controlled with an Oxford Cryostream cryostat. Diffraction intensities were obtained by azimuthal integration using the Fibrefix program (CCP13 suite) and were Lorentz and multiplicity corrected.

3 Results and discussion

Novel inclusion complexes, based on coordination and particular affinity for sodium or potassium cations inside six-oxygen cavity, are presented in Scheme 1.

Scheme 1.

Thermogravimetric analysis (Fig. 1 and Table S1-supplementary data) obtained the most prominent decrease in mass for both of the sodium-containing systems between 423 and 523 K, and for compound **3** between 523 and 573 K. In the case of system **2**, this is attributable to decomplexation of the 18C6 crown from sodium. In the case of complex **1** and **3**, however, decrease in mass of 78 % and 85 %, respectively, is not explainable by decomplexation only, but also with simultaneous decomposition of the anion. DTA curve of complex **1**, shows two minima in the 473-523 K region, one at 478 K and another at 495 K. Considering the formula of the sample, this decrease could be explained with dealkylation of the DS anion, which leads to the formation of sodium sulfate, confirmed by infrared spectrum of the sample after heating to 453 K. Above the temperature of 523 K, further decrease in mass is attributed to pyrolysis of the DS and DBS anion, respectively. For compound **3**, a negative peak occurs at 485 K, which suggests decomplexation of the crown, followed with a very intensive positive peak at 566 K, which might be explained with decomposition of picrate anion (not observed by infrared spectroscopy, IR).

Table 1 shows transition temperatures, T/K , enthalpies, $\Delta H/kJ\ mol^{-1}$, and entropies, $\Delta S/J\ mol^{-1}\ K^{-1}$, during heating and cooling cycles of examined compounds **1** – **3**. Although two different types of complexes are considered, first with sodium and second with potassium cations, the difference can also be noticed among anionic constituents. The micrographs (Fig. 2) refer the behavior of compounds **1** and **2** as Sm liquid crystalline; but **3** as crystalline. Fig. 3 and Table 2 contain the diffractograms of the samples **1** and **2** recorded at different temperatures. Thermal changes on the molecular level as well as thermodynamic parameters of decomplexation were explained with temperature-dependent IR spectroscopy. Fig. S1 (supplementary data) and Table 3 contain the most important functional groups assigned to IR spectral features at room temperature. Decomplexation enthalpy and entropy changes

were obtained from the absorbance measurement of complexed and decomplexed sodium salts. The detailed calculations are explained in Supplementary data S2 and shown in Fig. S2, while parameters obtained by linear fitting of the data are given in Table 1.

System **1** is crystal at room temperature (Fig. 2, 1a) with a bilayer-like arrangement and lamellar thickness of 38.56 Å (Fig. 3, upper part, right, Table 2). The crystal smectic (Sm) layer is composed of repetitive units of two crown ether layers with extended dodecyl chains. When untreated sample is chilled from room temperature to 265 K, slightly striated, smooth fan-like textures are formed (Fig. 2, 1c), characteristic for SmA, and confirmed by the SAXS (Fig. 3, upper part, left). This phase is composed of the layers with repetitive units of two crown layers and one layer of interdigitated dodecyl chains. Specificity of this system is relative fragility of the S-O-C linkage in *n*-dodecylsulfate anion. As previously considered by TGA, dodecyl moiety is abstracted from the system simultaneously with crown ether. From variable-temperature IR spectra (Fig. 4a) it is confirmed that 453 K spectrum corresponds to spectrum of sodium sulfate [29]. When heated from room temperature, sample **1** (Fig. 2, 1a-b, Table 1) exhibits solid-liquid crystalline transformation at 382 K, characterized by a double refracting lancets and pseudoisotropic regions, indicating most probably SmB mesophase that is stable until melting accompanied with beginning of decomposition, confirmed by temperature dependence of the baseline absorption at 2500 cm⁻¹ (Fig. 4b). A sharp transition in the interval 393-413 K with temperature of 401 K characterizes diffusion of the crown ether from the sample. The second transition is a milder step at 425 K and is solved with the help of temperature behavior of the spectral features due to the crown and dodecyl group (Fig. 4c). The band at 1109 cm⁻¹ is due to the $\nu(\text{C-O})$, which directly binds Na⁺ [30], strongly overlapped with sulfate anion stretching, and with the feature at 1195 cm⁻¹ that arises above 403 K. 960 cm⁻¹ and 836 cm⁻¹ absorption that correspond to the deformation vibrations of CH groups [30] also show dependence characteristic for both processes. However, a relatively linear shape of the first step, together with linearity of the absorbance over the whole temperature range, indicates that crown decomplexation and diffusion from the system occurs over the completely considered temperature range, while dodecyl group is detached in the 408-438 K range. More information given by the IR spectroscopy is in Supplementary data S3 and Fig. S3.

The soft anhydrous sample **2** shows properties similar to those of sample **1**, but it is also very specific. Microscopic examinations during heating detected only changes of textures at 318 K, seen as Maltese crosses (Fig. 2, 2a). Contrary to this, after the sample was chilled for 24 hours, the smooth fan-like textures characteristic for SmA phase were obtained (Fig. 2, 2b). Shorter time of cooling or gentle temperature elevation results with changed and disturbed pseudoisotropic spherulitic phase (Fig. 2, 2c). Although WAXS measurement evidences no order (Fig. 3, bottom, left), SAXS measurement of the sample kept in freezer for several hours indicates the most probably short-range, layer-like order (Fig. 3, bottom, right), with the diffuse peak corresponding the lamellar thickness of 29.7 Å. The similar values of lamellar thicknesses of sample **1** and **2** indicate the minor role of the benzene ring, but at the same time confirm disordering abilities of 4-(1-pentylheptyl)benzenesulfonate anion. This is in accordance with sulfonate hydrotropic properties; they are defined as amphiphilic molecules that cannot form well organized structures, cause microstructural changes, decrease membrane stability [31], disrupt lamellar liquid-crystalline phase, alter macroscopic properties [32,33]. Based on crystal structure analysis, these compounds form open-layer assemblies, consisting of clustered non-polar regions, adjacent to ionic polar regions, knitted together in a two-dimensional network, where stacking of aromatic ring is not detected [1].

Thermodynamic parameters of compound **2** (Table 1) point out relatively low transition temperatures during heating cycle. The first is for solid-liquid crystal transition, followed by a weak endothermic process, for which parameters may imply as Sm polymorphic transition, capacitance of possible moisture content or volume changes. The third one, at 265 K is the liquid crystal-isotropic liquid transition. Dependence of the baseline absorption at 2500 cm⁻¹ shown in Fig. 5a presents the next transition temperature (404 K), determined by differentiation of the absorbance, and fitting to fourth order polynomial. Again, the decomplexation of the crown occurs with its consequent diffusion from the sample, and the absorption due to the sulfate moiety remains constant over the considered temperature range. Variable-temperature IR spectra for system **2**, together with detailed description of the adequate bands for sulfate moiety and crown feature are in the Supplementary data S4 and Fig. S4.

The crystal structure of compound **3** with triclinic space group $P\bar{1}$ was solved earlier by Barnes and Collard [34]. However, systematic thermochemical study of this complex has never been performed. As seen from Table 2, it undergoes crystal – crystal polymorphic phase transitions that are not visible with microscope, until 473 K, when melting occurs (Fig. 2, 3b) and parallel, partial decomposition is involved. TG suggests that crown decomplexation occurs simultaneously with decomposition of picrate. However, temperature-dependent infrared baseline absorption at 2500 cm^{-1} (Fig. 5b) clearly resolves two processes, with transition temperatures of 445 K and 490 K, respectively. In order to extract information on decomplexation, the absorption in $3000\text{-}2650\text{ cm}^{-1}$, which arises due to the $\nu(\text{CH})$, was considered. In this region, a rather complex absorption occurs. Therefore, we have fitted only the absorption at 2830 cm^{-1} to Lorentzian profile function, as shown in the inset of Fig. 5b. It is evident that decomplexation occurs in two steps. Since the boiling point of crown 18C6 is 389 K, both steps include decomplexation and diffusion of free crown. Thus, we rather attribute the difference in behavior to two phases, with a phase transition at 461 K. However, this phase transition is not observed in temperature dependence of baseline absorption. At least for this moment, this difference remains unresolved. Melting point of potassium picrate is 520 K. From this fact, it is evident that in the temperature range 483-523 K, which is characterized by abrupt increase in baseline absorption, constant absorption at 2830 cm^{-1} , and only a minor decrease in mass for TG, large structural changes due to the phase transformation occur before melting. Variable-temperature IR spectra for **3** is shown in Fig S5 in Supplementary data S5 with clear explanation of thermal behavior.

4 Conclusions

Complexes based on 18C6 ether were synthesized and studied in terms of their thermal and structural properties. The present data point out that starting from aqueous 18C6-anionic surfactant solutions along with electrostatic interactions; hydrophobic interactions assist in a favorable way the molecular recognition properties. A strong entrapment of the organic surfactant guests of miscellaneous geometries into macrocyclic cation receptor, results in solid compounds that self-assemble in aggregates with wide spectrum of their physico-chemical characteristics. The properties of novel 18C6 complexes are function of anionic molecule geometry, type of chosen cation (Na^+ , K^+), as well as architecture of self-organized structures. The strength of coordination between Na^+ and oxygen atoms of 18C6 ligand does not depend on anionic part of the surfactant.

Synthesized coordination complexes are specific due to their different endothermic transitions. Enthalpy and entropy values of thermal transitions point to mesomorphous behavior of 18C6-NaDS and 18C6-NaDBS, confirmed with PXRD. Maltese crosses and smooth fan-like textures, characteristic for smectic A phase, and double refracting lancets *i.e.* smectic B mesophase, were obtained for 18C6-NaDS, which is also crystal smectic at room temperature. 18C6-NaDBS is characterized as compound of low melting point, forming smectic A phase during heating cycle. These results are valuable proofs that anionic surfactant molecule acts as promoter of thermotropic mesomorphism. The similar values of lamellar thicknesses of the 18C6-NaDS and 18C6-NaDBS indicate the minor role of the benzene ring size, but at the same time confirm disordering abilities of 4-(1-pentylheptyl)benzenesulfonate anion. Temperature of the decomplexation of 18C6-KP is considerably higher than of 18C6-NaDS and 18C6-NaDBS, and distortion of 18C6-NaDS and 18C6-KP complexes occurs in two steps. A good combination of crown ether unit and amphiphile may provide a possibility for preparing new functionalized materials, opening the research field of ion complexation and of host-guest type behavior. Many of material applications benefit from similar arrangements with 18C6, controlled formation of ordered mesomorphous and three-dimensional crystal structures.

Acknowledgment.

This work has received support from the Ministry of Education, Science and Sport of the Republic of Croatia (Project No. 098-0982915-2949, 098-0982904-2927 and 098-0982904-2941).

References

- [1] N.V. Markova, V.P. Vasiliev, Thermochemistry of 18C6 complexation with alkali, alkaline earth metal cations and ammonium ion, *J. Therm. Anal.* 45 (1995) 695–701.
- [2] S. De, Preferential interaction of charged alkali metal ions (guest) within a narrow cavity of cyclic crown ethers (neutral host): A quantum chemical investigation, *J. Mol. Struct.* 941 (2010) 90–101.
- [3] P. Tomar, R. Kolhapurkar, D. Dagade, K. Patil, Equilibrium Constant Studies for Complexation between Ammonium Ions and 18-Crown-6 in Aqueous Solutions at 298.15 K, *J. Solution Chem.* 36 (2007) 193–209.
- [4] Doxsee K.M., Francis P.E., Weakley T.J.R., Hydration, Ion Pairing, and Sandwich Motifs in Ammonium Nitrate Complexes of Crown Ethers, *Tetrahedron.* 56 (2000) 6683–6691.
- [5] G. Unruh, J. Cumbest, Crown Ethers Enhance Ionic Residue Removal, *Res. Develop.* (1994).
- [6] B.A. Moyer, J.F. Birdwell, P.V. Bonnesen, L.H. Delmau, Use of Macrocycles in Nuclear-Waste Cleanup: A Realworld Application of a Calixcrown in Cesium Separation Technology, in: K. Gloe (Ed.), *Macrocyclic Chemistry*, Springer-Verlag, Berlin/Heidelberg, n.d. pp. 383–405.
- [7] I.A. Darwish, I.F. Uchegbu, The evaluation of crown ether based niosomes as cation containing and cation sensitive drug delivery systems, *Int. J. Pharm.* 159 (1997) 207–213.
- [8] R. Muzzalupo, F.P. Nicoletta, S. Trombino, R. Cassano, F. Iemma, N. Picci, A new crown ether as vesicular carrier for 5-fluoruracil: synthesis, characterization and drug delivery evaluation, *Colloids Surf. B, Biointerfaces.* 58 (2007) 197–202.
- [9] D. Cram, Synthetic host-guest chemistry, in: *Applications of Biochemical Systems in Organic Chemistry*, J. B. Jones, C. J. Sih, D. Perlman, Wiley, New York, NY, USA, 1976: p. 815.
- [10] R. Berezcki, B. Ágai, I. Bitter, Synthesis and Alkali Cation Extraction Ability of New Mono and Bis(benzocrown ether)s with Terminal Alkenyl Groups, *J. Inclusion Phenom.* 47 (2003) 53–58.
- [11] M. Nakajima, K. Kimura, T. Shono, Liquid chromatography of alkali and alkaline earth metal salts on poly(benzo-15-crown-5)- and bis(benzo-15-crown-5)-modified silicas, *Anal. Chem.* 55 (1983) 463–467.
- [12] A. Wong, G. Wu, Solid-State ^{23}Na Nuclear Magnetic Resonance of Sodium Complexes with Crown Ethers, Cryptands, and Naturally Occurring Antibiotic Ionophores: A Direct Probe to the Sodium-Binding Sites, *J. Phys. Chem. A.* 104 (2000) 11844–11852.
- [13] K.J. Koch, T. Aggerholm, S.C. Nanita, R.G. Cooks, Clustering of nucleobases with alkali metals studied by electrospray ionization tandem mass spectrometry: implications for mechanisms of multistrand DNA stabilization, *J. Mass Spectrom.* 37 (2002) 676–86.
- [14] J.C. Chaput, C. Switzer, A DNA pentaplex incorporating nucleobase quintets, *Proceedings Nat. Ac. Sci.* 96 (1999) 10614–10619.
- [15] Y. Kudo, S. Katsuta, Y. Takeda, Potentiometric Determination of the Ion-Pair Formation Constant of a Univalent Cation-Neutral Ligand Complex with an Anion in Water Using an Ion-Selective Electrode, *Anal. Sci.* 15 (1999) 597–599.
- [16] C. Danumah, Siliceous mesoporous molecular sieves derived from crown ether surfactants, *Microporous Mesoporous Mater.* 37 (2000) 21.
- [17] N. Steinke, M. Kaller, M. Nimtz, A. Baro, S. Laschat, Columnar liquid crystals derived from crown ethers with two lateral ester-substituted ortho-terphenyl units: unexpected destabilisation of the mesophase by potassium iodide, *Liq. Cryst.* 37 (2010) 1139–1149.
- [18] A. Schultz, S. Laschat, A. Saipa, F. Gießelmann, M. Nimtz, J.L. Schulte, et al., Columnar Liquid Crystals with a Central Crown Ether Unit, *Adv. Funct. Mater.* 14 (2004) 163–168.
- [19] J. Goodby, G. Mehl, I. Saez, R. Tuffin, G. Mackenzie, R. Auzely-velty, et al., Liquid Crystals with Restricted Molecular Topologies: Supermolecules and Supramolecular Assemblies, *Chem. Inform.* 29 (1998) 2057–2070.
- [20] K. Leblanc, P. Berdagué, J. Rault, J.-P. Bayle, P. Judeinstein, Synthesis and ionic properties of nematic compounds bearing an ether-crown moiety: an NMR approach, *Chem. Commun.* (2000) 1291–1292.

- [21] Y. Nishikawa, T. Watanabe, H. Yoshida, M. Ikeda, Phase transition behaviors of crown-ether derivative and its sodium ion complex, *Thermochim. Acta.* 431 (2005) 81–86.
- [22] M. Kaller, S. Laschat, Liquid Crystalline Crown Ethers, in: C. Tschierske (Ed.), *Liq. Cryst.*, Springer Berlin Heidelberg, Berlin, Heidelberg, 2011: pp. 109–192.
- [23] D.S. Nagvekar, Y. Delaviz, A. Prasad, J.S. Merola, H. Marand, H.W. Gibson, Synthesis and Properties of Cholesteryl Esters Bearing 32- and 16-Membered Crown Ethers, *J. Org. Chem.* 61 (1996) 1211–1218.
- [24] G.X. He, F. Wada, K. Kikukawa, S. Shinkai, T. Matsuda, Syntheses and thermal properties of new liquid crystals bearing a crown ether ring: cation binding in the nematic phase, *J. Org. Chem.* 55 (1990) 541–548.
- [25] L. Bereczki, K. Marthi, P. Huszthy, G. Pokol, 18-crown-6 ether complexes with aralkylammonium perchlorates, *J. Therm. Anal. Calorim.* 78 (2004) 449–459.
- [26] T. Mihelj, V. Tomašić, Amphiphilic Properties of Dodecylammonium Chloride/4-(1-Pentylheptyl) Benzene Sodium Sulfonate Aqueous Mixtures and Study of the Catanionic Complex, *J. Surfact Deterg.* 2013, DOI 10.1007/s11743-013-1504-y.
- [27] Y. Kudo, M. Wakasa, T. Ito, J. Usami, S. Katsuta, Y. Takeda, Determination of ion-pair formation constants of univalent metal-crown ether complex ions with anions in water using ion-selective electrodes: application of modified determination methods to several salts, *Anal. Bioanal. Chem.* 381 (2004) 456–463.
- [28] Y. Kudo, J. Usami, S. Katsuta, Y. Takeda, Solvent extraction of silver picrate by 3m-crown-m ethers ($m = 5, 6$) and its mono-benzo-derivative from water into benzene or chloroform: elucidation of an extraction equilibrium using component equilibrium constants, *Talanta.* 62 (2004) 701–706.
- [29] A. Periasamy, S. Muruganand, M. Palaniswamy, Vibrational studies of Na₂SO₄, K₂SO₄, NaHSO₄ AND KHSO₄ crystals, *Rasayan J. Chem.* 2 (2009) 981–989.
- [30] Cooper, Infrared Spectroscopy of Divalent Zinc and Cadmium Crown Ether Systems, *J. Phys. Chem. A.* 115 (2011) 5408–5422.
- [31] P. Wieczorek, Factors influencing the transport of tryptophan hydrochloride through supported liquid membranes containing macrocyclic carriers, *J. Membr. Sci.* 127 (1997) 87–92.
- [32] T.K. Hodgdon, E.W. Kaler, Hydrotropic solutions, *Curr. Opin. Colloid Interface Sci.* 12 (2007) 121–128.
- [33] R. Guo, M.E. Compo, S.E. Friberg, K. Morris, The Coupling Action of a Hydrotrope and Structure Transition from Lamellar Liquid Crystal, *J. Dispersion Sci. Technol.* 17 (1996) 493–507.
- [34] J. Barnes, J. Collard, 18-Crown-6-potassium picrate (1/1), *Acta Crystallogr., Sect. C: Cryst. Struct. Commun.* 44 (1988) 565–566.

Tables

Table 1 Transition temperatures, T/K , enthalpies, $\Delta H/kJ\ mol^{-1}$, and entropies, $\Delta S/J\ mol^{-1}\ K^{-1}$ of examined **1 – 3** compounds given by the DSC measurements, with thermodynamic functions for decomplexation of 18C6 from synthesized compounds, given by the temperature-dependent IR measurements (bold).

Compound	Heating			Cooling
	T/K	$\Delta H/kJ\ mol^{-1}$	$\Delta S/J\ mol^{-1}\ K^{-1}$	
1	382.12	2.55	6.67	Decomposition
	398.30	9.14	22.96	
	401.00	93.30	236.10	
2	241.19	1.94	7.85	No transitions detected
	257.60	0.55	2.12	
	269.05	0.39	1.46	
	404.00	81.80	206.30	
3	328.06	22.76	69.38	Partial decomposition
	345.66	4.34	12.56	
	388.85	23.28	59.87	
	472.57	47.94	101.45	
	461.00	164.10	358.40	

Table 2 Interplanar spacing, d , Miller indices, hkl , and relative intensities I_{rel} , for compound **1** at room temperature.

$d/\text{\AA}$	hkl	I_{rel}
38.56	*001	>100
19.28	002	92.7
12.89	003	100
9.68	004	1.7
7.75	005	3.5
6.46	006	4.6
4.84	008	1.4
4.35	009	0.4
2.76	0,0,14	0.1
2.58	0,0,15	0.1

* calculated

Table 3 Assignment of the infrared spectra of the complexes.

Compound 1	Compound 2	Compound 3	Assignment
3463	3453	3450	Water
3402			Crown
		3100	Picrate $\nu(\text{CH})$
		3081	Picrate $\nu(\text{CH})$
2955	2956	2952	Crown
	2925		$\nu(\text{CH})$
2917		2909	Crown
		2888	Crown
2853	2857	2862	Crown
2824		2831	Crown
		1977	Picrate $\delta(\text{CH})$ overtone
			$\nu(\text{COO} \cdots \text{H}_2\text{O})$
		1635	
		1613	
		1566	
		1557	
		1512	
1472	1469	1479	Crown
1456	1457	1457	Crown
1432		1437	Crown
		1365	
1351	1351	1353	Crown
		1334	
		1311	
		1289	Crown
1280	1284	1272	Crown
1249	1248	1256	Crown
1227			Alkyl
1222	1218		C-S
	1193		NaHSO ₄
		1164	Picrate $\nu(\text{C-O})$
		1136	
1107	1108	1112	Crown; DS and DBS SO ₄ group; picrate $\nu(\text{CO})$
1082			Alkyl
		1074	
	1038		Benzene ring
1019	1011		C-S
997			
965	965	964	Crown
921			
		910	
		872	Picrate
837	837	837	Crown
		787	
764			
		741	
721			
		708	Picrate
635			
		600	Picrate $\delta(\text{C-NO}_2)$
590	584		Crown
		537	Crown
528	530	526	Crown
468	470	515	Crown

Figures

Scheme 1. The scheme of the examined complexes: 18C6-sodium *n*-dodecylsulfate (compound **1**), 18C6-sodium 4-(1-pentylheptyl)benzenesulfonate (**2**), and 18C6-potassium picrate (**3**) complex.

Fig. 1. Thermograms (straight line) and DTA results (dashed line) for compound **1** (**a**), **2** (**b**) and **3** (**c**).

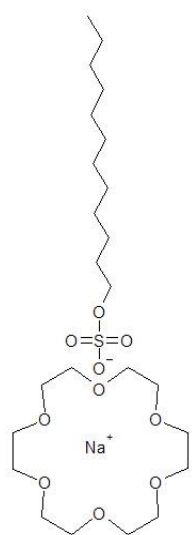
Fig. 2. The micrographs of the characteristic textures of the examined samples **1** – **3** taken at different temperatures in heating (h) and cooling (c) cycle, as observed by the optical microscope under crossed polarizers. The bar represents 250 μm (**1a**, **1b**, **1d**, **2a**, **3b** and **3c**), 100 μm (**1c**, **2b**), and 50 μm (**1e**, **2c** and **3a**). The temperatures, T/K , are as indicated.

Fig. 3. WAXS diffractograms recorded at room temperature (left) and SAXS diffractograms at lower temperatures (right) of the samples **1** (upper part) and **2** (bottom).

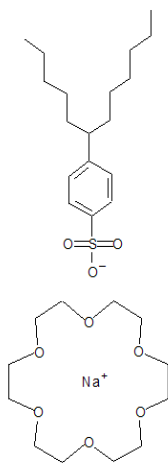
Fig. 4. Baseline corrected variable-temperature infrared spectra for compound **1** in the 373-453 K interval (**a**). Temperature dependence of the baseline absorption at 2500 cm^{-1} . Inset shows the first derivative of the curve for the purposes of determination of the transition temperatures (**b**). Temperature dependence of the characteristic 836 cm^{-1} band (**c**).

Fig. 5. Temperature dependence of the baseline absorption at 2500 cm^{-1} for system **2**. Inset shows the first derivative of the curve and fit to 4th order polynomial for the purposes of determination of the transition temperature (**a**). Temperature dependence of the baseline absorption 2500 cm^{-1} for system **3**. Inset shows the first derivative of the curve (2830 cm^{-1} band) and fit to two gaussian functions for the purposes of determination of the transition temperatures (**b**).

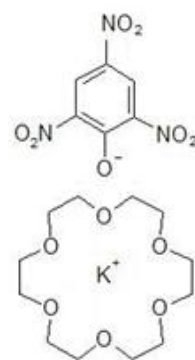
Scheme 1.



1

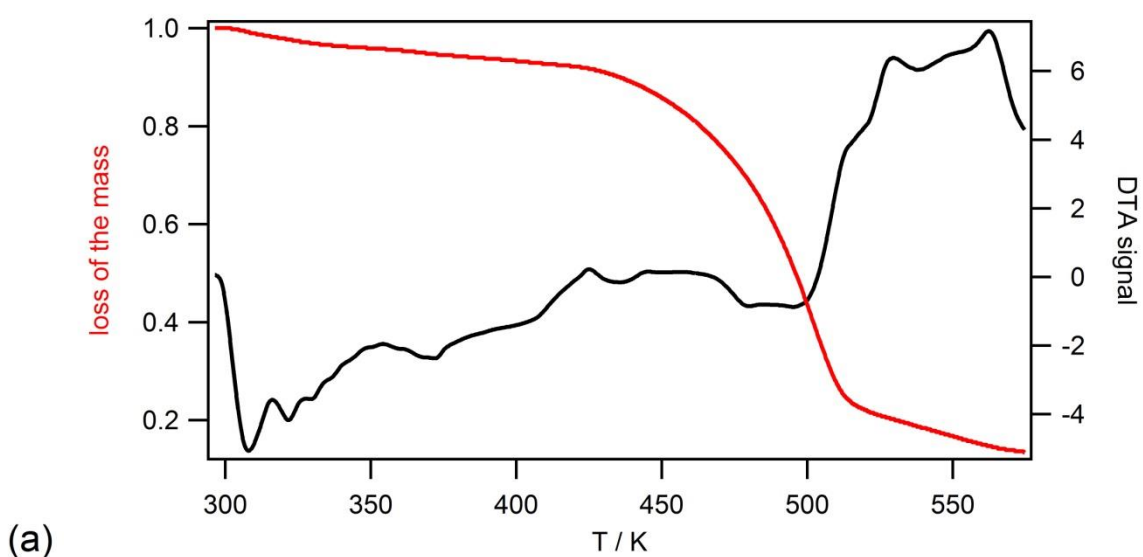


2

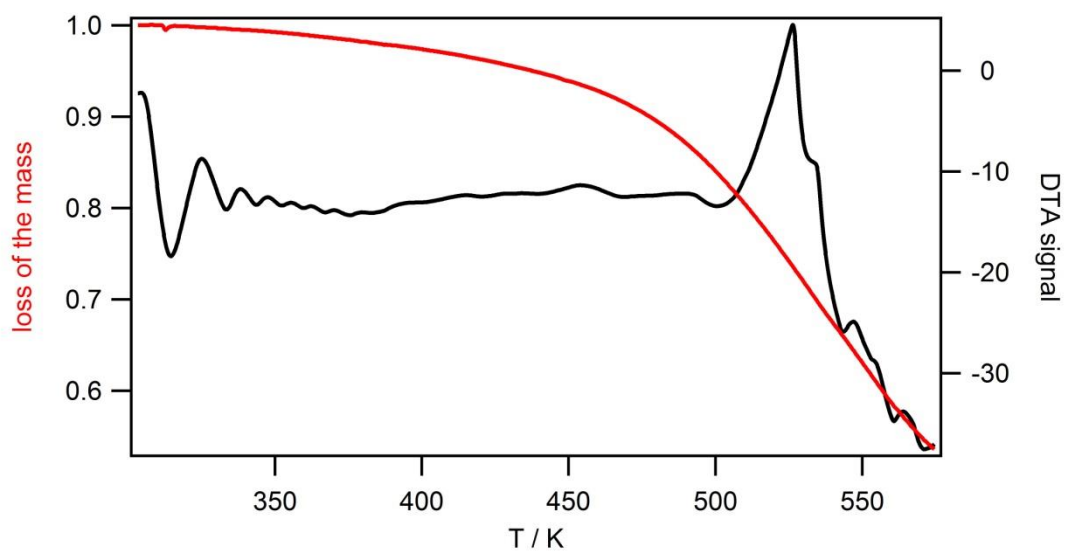


3

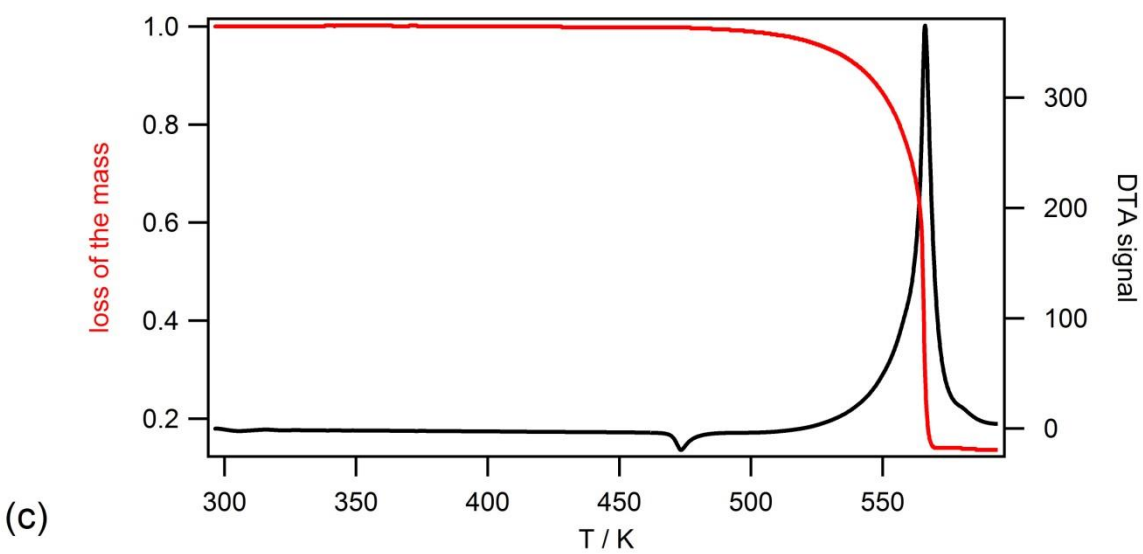
Fig. 1.



(a)



(b)



(c)

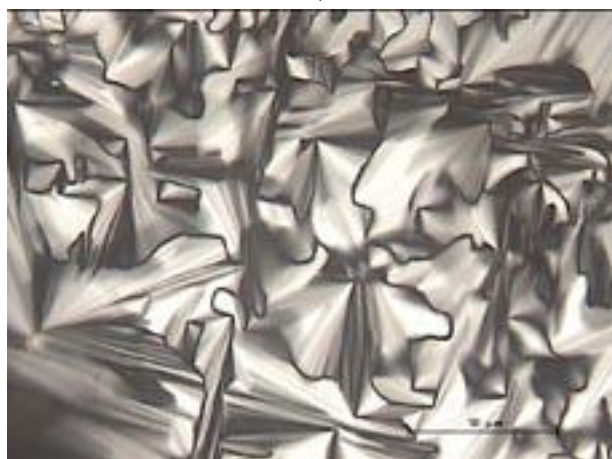
Fig. 2.



1a, 298 K



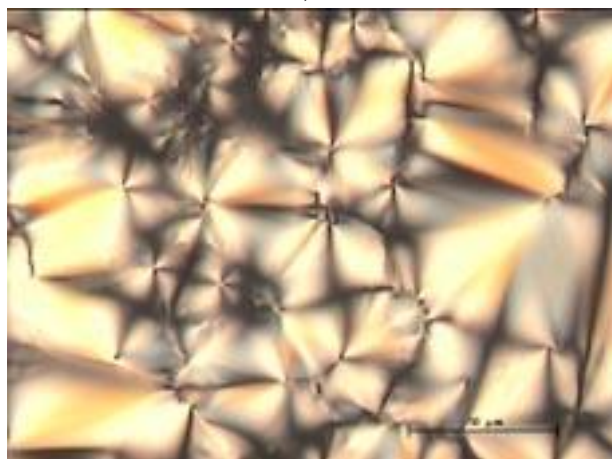
1b, h: 385 K



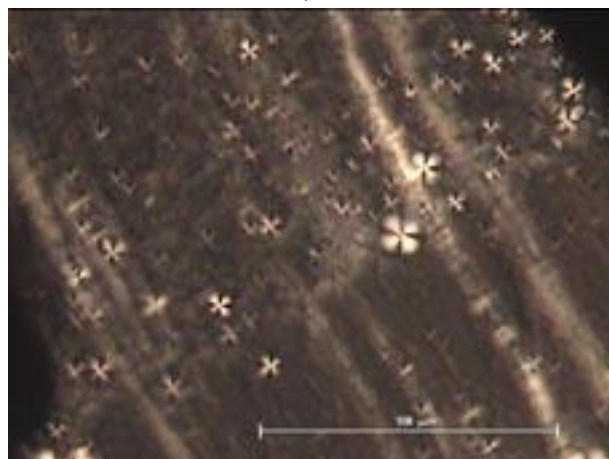
1c, c: 265 K



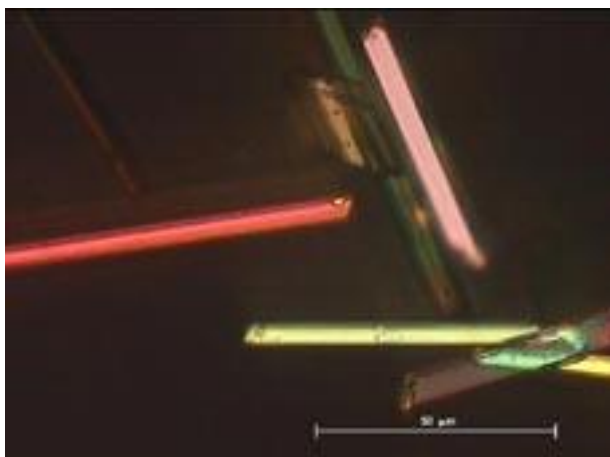
2a, h: 318 K



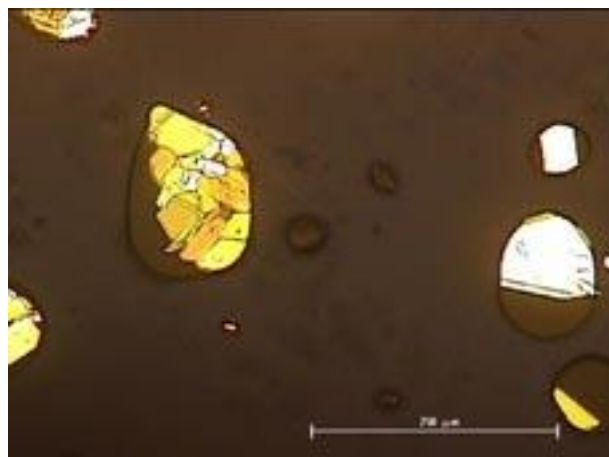
2b, c: 243 K, 24 hours



2c, c: 243, 12 hours

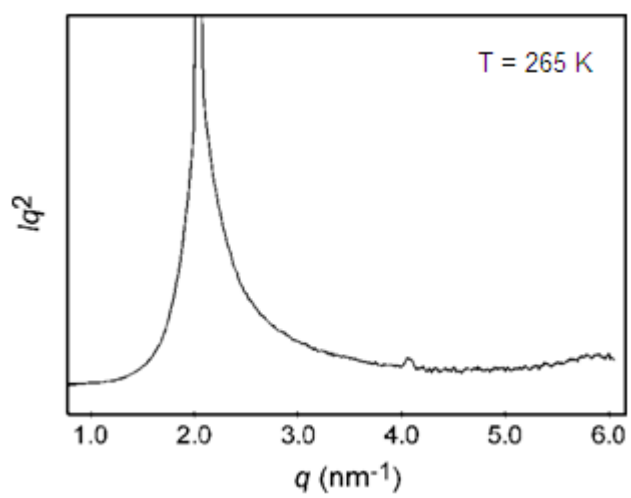
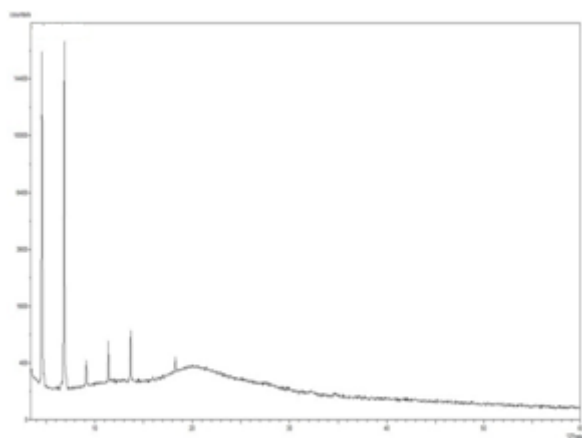


3a, h: 318 K

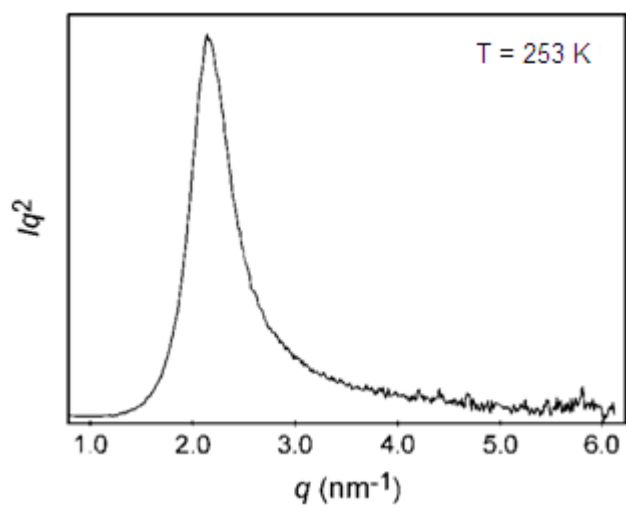
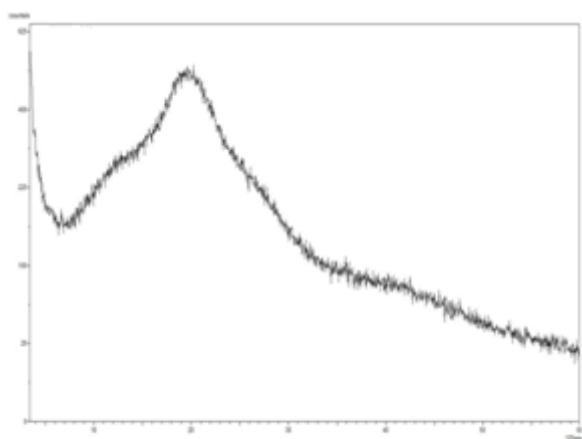


3b, h: 473 K

Fig. 3.

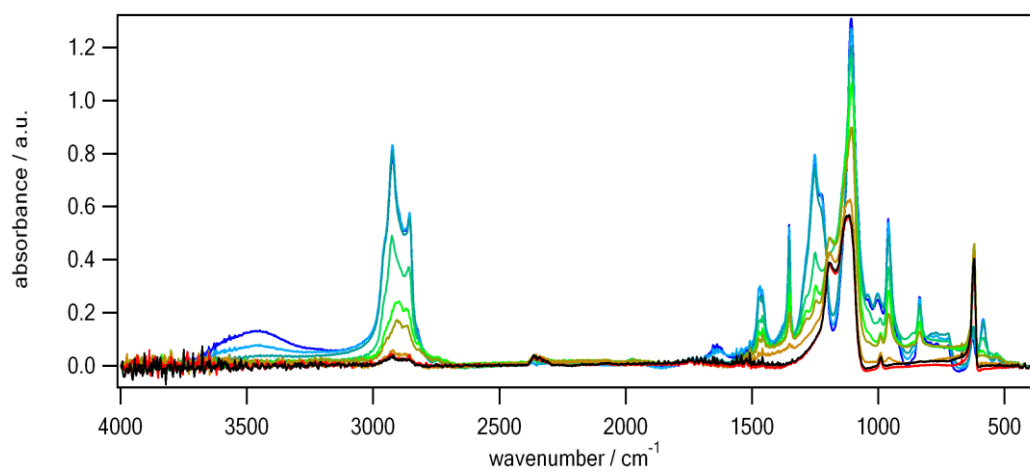


1

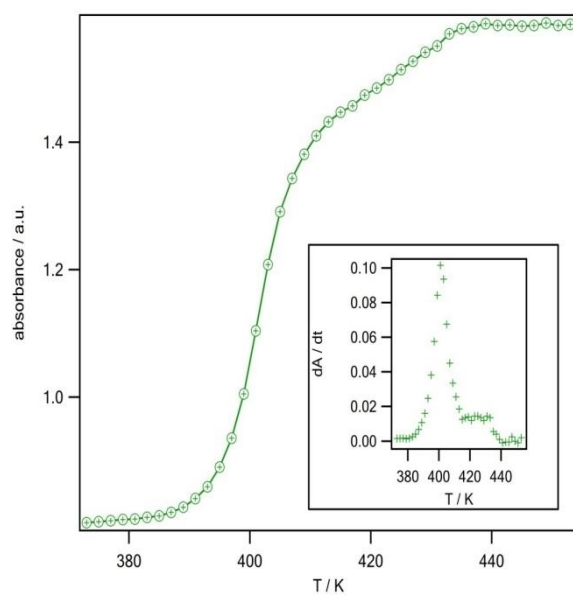


2

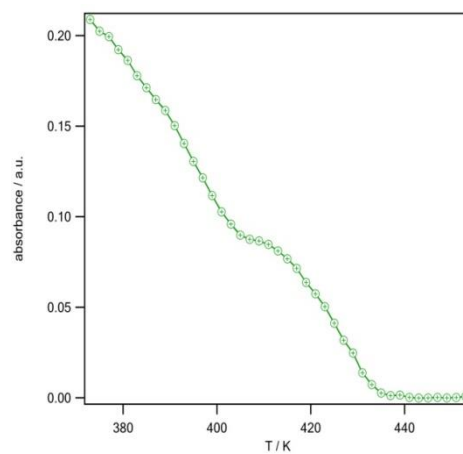
Fig. 4.



a

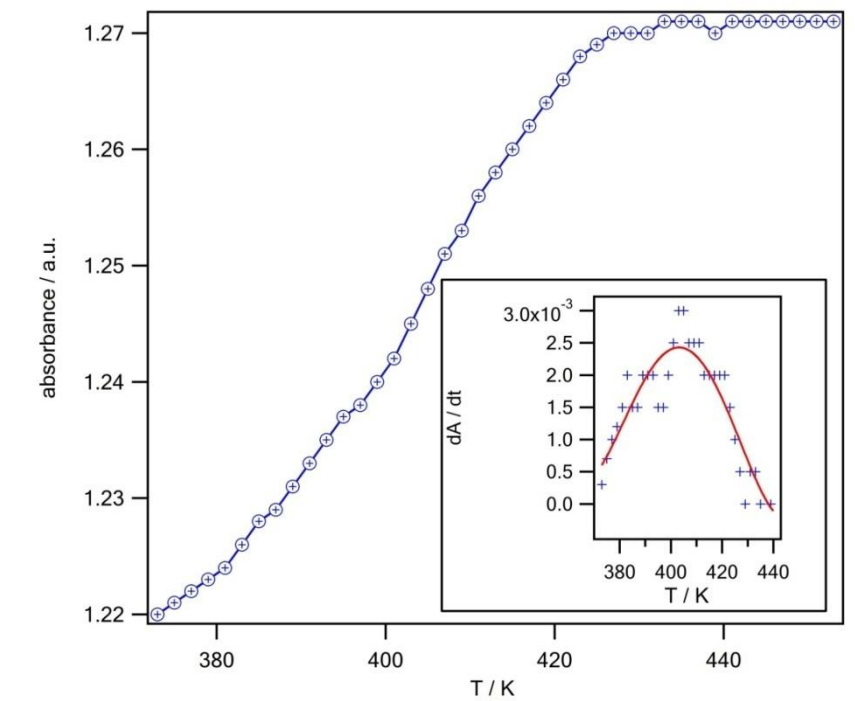


b

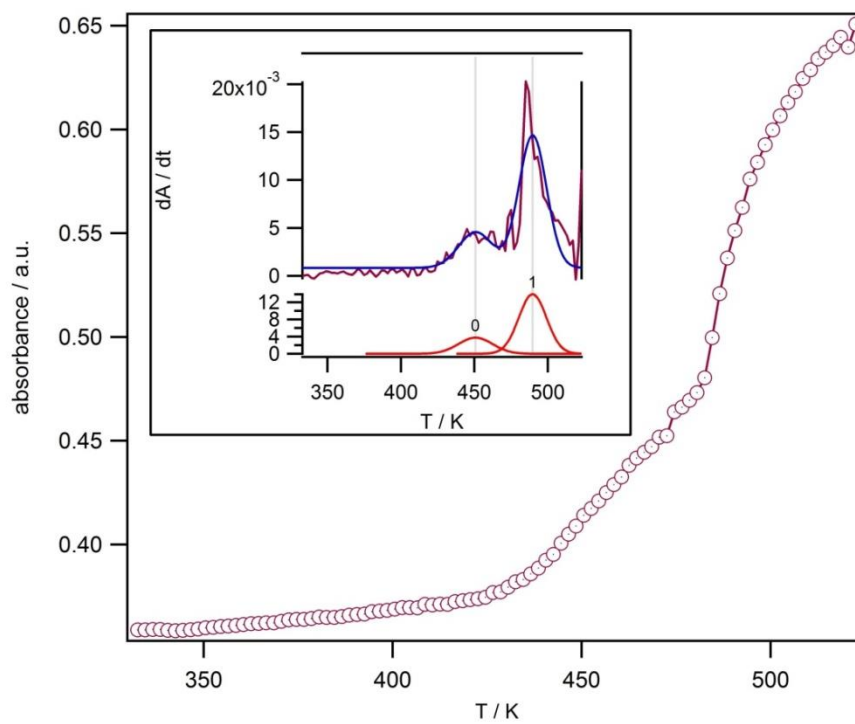


c

Fig 5.



a



b